Modelling the effect of surgical stress and bacterial growth in human cornea
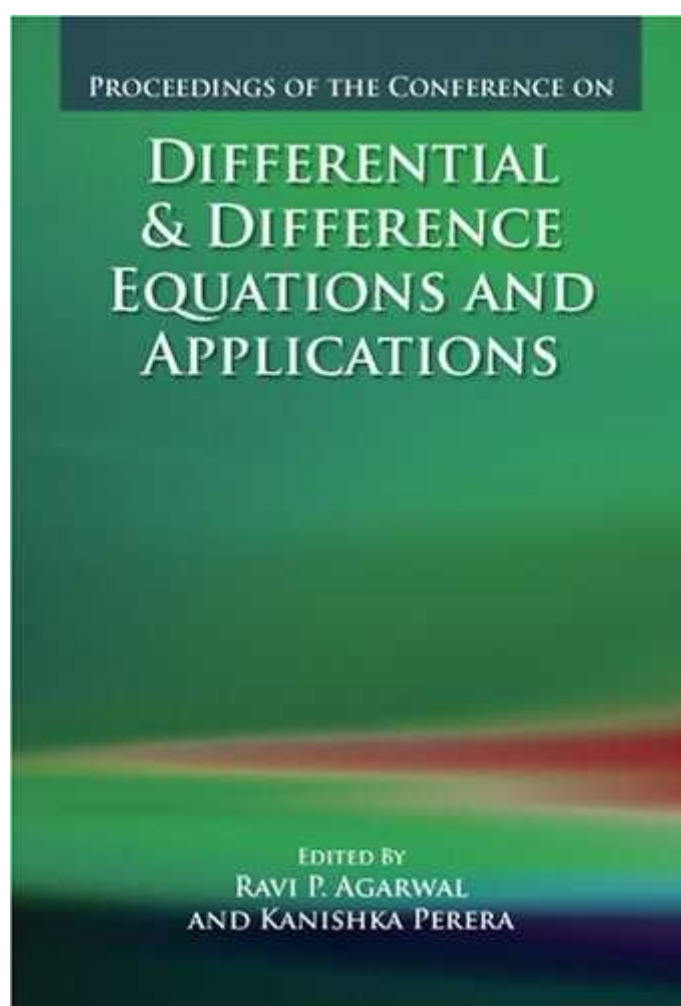
Mahapatra, D.R. and Melnik, R.V.N.

MODELLING THE EFFECT OF SURGICAL STRESS AND BACTERIAL GROWTH IN HUMAN CORNEA

D. ROY MAHAPATRA AND R. V. N. MELNIK

This paper reports a mathematical model and finite-element simulation of the dynamic piezoelectricity in human cornea including the effect of dehydration and stress generated due to incision and bacterial growth. A constitutive model is proposed for the numerical characterization of cornea based on the available experimental data. The constitutive model is then employed to derive the conservation law for the dynamic piezoelectricity supplemented by the time-dependent equation for the electromagnetic field. The resulting system of partial differential equations is solved numerically with finite-element methodology. Numerical results presented here demonstrate promising applications of the developed model in aiding refractive surgery and a better understanding of regenerative processes in cornea.

1. Introduction

Cornea is one of the most delicate and active tissue systems in human and several other species. Any major change in the equilibrium stress in the sclera and cornea due to incision, excessive swelling, and bacterial growth can cause deterioration of the refractive performance of the cornea. Cornea consists of a complex architecture of the collagen fibrils dispersed in the matrix containing proteoglycans. The anisotropic structure of this composite system is distributed over the stromal layer. Computer models for surgical aid in the past had been developed, these models neglected the effect of complex tissue architecture and the resulting constitutive behavior in the long-term tissue remodelling. The role of these factors in context of surgical procedures has been brought into focus only recently and mathematical model has been proposed (see [6]).

Apart from the collagen orientation-dependent anisotropy in cornea, it may be noted that the dynamic nature of the refractive property, which is very little understood in the case of cornea as compared to the sclera, is dependent on the electrical permittivity,

magnetic permeability, and the piezoelectric constants of the cell-matrix composition. Complication arises because of the piezoelectricity of collagen tissue. Mechanics of collagen tissue in corneal fibroblast has been studied extensively by several researchers. Petroll et al. [5] studied the correlation between the movement of cell-matrix adhesion sites and the force generation in corneal fibroblasts. A detailed discussion of the mechanism of cell-regulated collagen tissue remodelling in stromal fibroblasts can be found in the work of Girard et al. [3]. The experimental studies indicate a strong influence of stress-induced charge transport on the site-specific remodelling of the collagen structure in cornea. The resulting piezoelectricity is due to anisotropy of the collagen lattice [2, 8]. In cornea, stroma is the basic collagen fibril structure over which the extrafibrilar matrix is found with significant anisotropy. The cell-matrix adhesion is mainly controlled by the cross-linking agent (proteoglycans) which are negatively charged. The complex structure transforms or breaks down due to change in the concentration of H_2O. Thus, the state of hydration and the anisotropy of collagen fibrils are two interlinked and important factors that affect the piezoelectric property and hence the long-term tissue remodelling in cornea under various environmental and surgical conditions. As a fundamental cause of piezoelectricity, the structural transformation in collagen during dehydration was reported by Pratzl and Daxer [7]. Although mathematical models for characterizing the collagen structure, as observed in the X-ray diffraction results, have been reported recently by Pinsky et al. [6], not many mathematical modelling studies are found in the literature which can be applied to characterize the influence of piezoelectricity on the delicate *dynamic* activity in cornea. Furthermore, it is highly desirable to incorporate the residual stress generation into new mathematical models when analyzing the bacterial growth-induced effects on the cornea.

Experimental studies of the influence of the directional effect of the collagen structure in human cornea have been carried out in the work of Jayasuriya et al. [4]. These studies show a significant influence of the orientation of the collagen fibers on the stiffness and the piezoelectric coefficients of the cell-matrix composition. Furthermore, the stiffness increases and the piezoelectric constants decrease as functions of the dehydration over time. Although the related experimental investigations involve specially prepared laboratory samples, in which the mechanical states of stress and deformation are already changed compared to that in living cornea, they essentially describe the long-term behavior of the mechanical and piezoelectric properties. Also, the anisotropic collagen structure in three dimensions is difficult to characterize experimentally and one can obtain only the correlated response using optical and X-ray measurements. Because of the above complexities, in order to provide a detailed characterization of the collagen structure and the resulting piezoelectricity, one requires comprehensive mathematical models that incorporate the important effects such as the anisotropy, the dehydration, and the small-scale dynamics of the cell-matrix adhesion.

In the present paper, we develop a mathematical model for the dynamic piezoelectricity of the corneal membrane and analyze the electric polarization of the composition due to circumferential stresses produced by bacterial growth or incision. The experimentally measured mechanical and piezoelectric properties reported in the work of Jayasuriya et al. [4] are used to construct the constitutive model. A mechanism of long-term
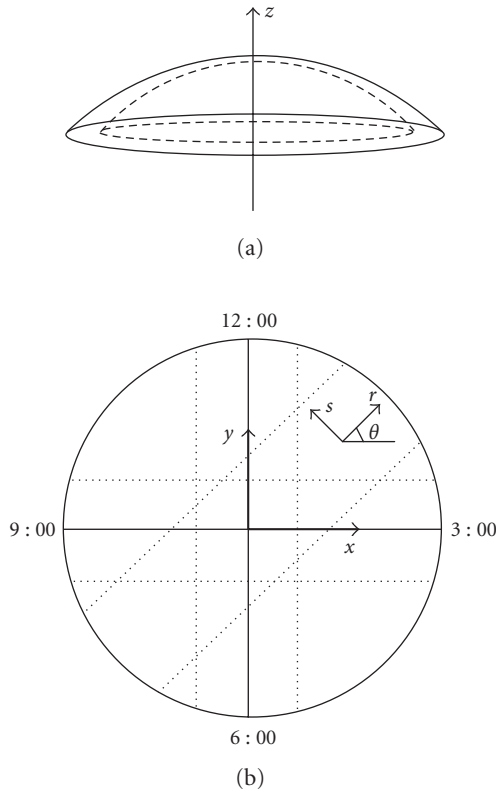
Figure 2.1. Schematic representation of (a) cornea model geometry and (b) angular orientation of the samples used in measuring the directional properties.

dehydration based on the experimental observations is included in the model. Coupling between the elastodynamics and the electromagnetics is dealt with in a systematic manner. A phenomenological approach to introduce the bacterial and antibiotic stress is discussed. Numerical results on the effect of circumferential stress is reported.

2. Constitutive model

Electromechanical characterization of the cornea tissue properties generally involves static and dynamic testing of samples with controlled state of dehydration and different cut angles (θ) from the cornea as schematically shown in Figure 2.1. In the published literature, some results on the corneal tissue invasive measurements are available, for example [4]. Such measurements are made by taking into consideration the effect of the cut angle θ on the anisotropic constitutive relation. They provide further insight into orthotropic properties (stiffness and piezoelectric constants) in the plane (x, y) assuming "no out-of-the-plane curvature." However, the collagen structure in various layers in the stroma and the type of anisotropy of the extrafibrilar structure are different. An experimental

electromechanical characterization of these differences would involve multiaxially controlled measurements which are not available at present in the published literature. Also, the site-dependence of the piezoelectric properties is most likely influenced by the presence of fibroblasts and cell-regulated processes. This would make the constitutive model dependent on the high-angle X-ray data (see discussions in [6]) that reveals the structural details as some function of (x, y, z), $z \in [h_i, h_0]$, where h_i and h_0 stand for the inner and the outer surfaces, respectively. However, at present, due to the lack of experimental data, we have not included such details in the developed mathematical model. Another important aspect is the variation of the electromechanical properties as functions of dehydration over time. In our proposed constitutive model, we introduce these details at the extent available from experimental observations.

Here, we first introduce a general mathematical setting for our problem. First we define the Cartesian components of stress ($\boldsymbol{\sigma}$), strain ($\boldsymbol{\varepsilon}$), electric charge displacement ($\boldsymbol{D}$), electric field intensity ($\boldsymbol{E}$), magnetic flux ($\boldsymbol{B}$), and the magnetic field intensity ($\boldsymbol{H}$) in (x, y, z). The general objective is to construct a constitutive model

$$\boldsymbol{\sigma} = \boldsymbol{c}\boldsymbol{\varepsilon} - \boldsymbol{\sigma}_p(\boldsymbol{E}), \tag{2.1a}$$

$$\boldsymbol{D} = \boldsymbol{\epsilon}\boldsymbol{E} + \boldsymbol{P}(\boldsymbol{\varepsilon}), \tag{2.1b}$$

$$\boldsymbol{B} = \boldsymbol{\mu}\boldsymbol{H} + \mu_0\boldsymbol{M}(\boldsymbol{\varepsilon}), \tag{2.1c}$$

where $\boldsymbol{c}$ is the stiffness, $\boldsymbol{\sigma}_p$ is the electric polarization induced stress, $\boldsymbol{\epsilon}$ is the dielectric permittivity, $\boldsymbol{P}$ is the electrical polarization vector due to transformation and deformation of the macromolecular structure, $\boldsymbol{\mu}$ is the magnetic permeability, and $\boldsymbol{M}$ is the magnetic polarization vector due to molecular spin. Splitting the total charge density ρ_{total} and the total conduction current $\boldsymbol{J}_{\text{total}}$ as

$$\rho_{\text{total}} = \rho_c + \rho_p, \qquad \boldsymbol{J}_{\text{total}} = \boldsymbol{J} + \boldsymbol{J}_p + \boldsymbol{J}_m, \tag{2.2}$$

where ρ_c is the true charge density, ρ_p is the bound charge density, $\boldsymbol{J}$ is the true conduction current, $\boldsymbol{J}_p$ is the conduction current due to bound charge, $\boldsymbol{J}_m$ is the molecular current density, we have the local conservation laws:

$$\nabla \cdot \boldsymbol{P} = -\rho_p, \qquad \nabla \times \boldsymbol{M} = \boldsymbol{J}_m, \tag{2.3}$$

and the local continuity condition

$$\nabla \cdot \boldsymbol{J}_p = -\dot{\rho}_p. \tag{2.4}$$

In order to characterize the constitutive mechanism that is likely to influence the refractive property most significantly, we consider the horizontal ($\theta = 0$), the vertical ($\theta = 90°$), and the diagonal ($\theta = 45°$) cuts as discussed in [4]. Dynamics of the horizontal cut sample involves (σ_{xx}, E_z) so that the longitudinal stiffness is obtained as

$$c_{11} = c_{11}^0 e^{t/\tau_1}, \quad \tau_1 > 0, \tag{2.5a}$$

and the piezoelectric coefficient under transverse electric polarization is obtained as

$$d_{31} = d_{31}^0 e^{t/\tau_1'}, \quad \tau_1' > 0, \tag{2.5b}$$

where the superscript 0 indicates the corresponding quantities at some initial state at time $(t = t_0)$ and τ_n, τ_n' (with $n = 1, 2, \dots$) are the time constants that are estimated from the time-resolved measurements of the corresponding quantities. Similarly, for the vertical cut, which involves (σ_{yy}, E_z), one can write

$$c_{22} = c_{22}^0 e^{t/\tau_2}, \quad \tau_2 > 0, \tag{2.6a}$$

$$d_{32} = d_{32}^0 e^{t/\tau_2'}, \quad \tau_2' > 0. \tag{2.6b}$$

With simple assumptions of aligned collagen fibers undergoing transverse electric polarization in the diagonal cut, which involves measurements in the transformed coordinate system (r, s, z) (see Figure 2.1), it is reasonable to write

$$\sigma_{rr} = c_{rr}\varepsilon_{rr} - d_{3r}E_z, \tag{2.7a}$$

$$c_{rr} = c_{rr}^0 e^{-t/\tau_3}, \quad \tau_3 > 0, \tag{2.7b}$$

$$d_{3r} = d_{3r}^0 e^{-t/\tau_3'}, \quad \tau_3' > 0, \tag{2.7c}$$

where

$$\sigma_{rr} = \sigma_{xx}\cos^2\theta + \sigma_{yy}\sin^2\theta - 2\sigma_{xy}\sin\theta\cos\theta, \tag{2.7d}$$

$$\sigma_{tt} = 0 = \sigma_{xx}\sin^2\theta - \sigma_{yy}\cos^2\theta - 2\sigma_{xy}\sin\theta\cos\theta, \tag{2.7e}$$

so that the orientation-dependent properties are obtained from experiments as

$$c_{12} = (c_{rr} - c_{11})\cot^2\theta, \qquad c_{21} = (c_{rr} - c_{22})\tan^2\theta, \tag{2.7f}$$

$$d_{36} = \frac{d_{3r} - d_{31}\cos^2\theta - d_{32}\sin^2\theta}{2\sin\theta\cos\theta}. \tag{2.7g}$$

Note that the properties estimated in this method are the effective properties of the composition. The underlying mechanism of viscopiezoelasticity may be postulated as follows. Let us consider a representative volume element (RVE) of the cell-matrix composition and assume that the volume fraction (v_h) of the fluid phase is governed by a convection-diffusion process and can be expressed as

$$v_h = v_h^0 e^{-t/\tau_0} \tag{2.8}$$

and the piezoelectricity is only due to the structural transformation of the collagen fibers. Then the true charge density can be approximated as

$$\rho_c = v_h e_h, \tag{2.9}$$

where e_h is the specific electric dipole. Equation (2.1a) takes the form

$$\boldsymbol{\sigma} = [v_h\boldsymbol{c}_h + (1-v_h)\boldsymbol{c}_f][1-\alpha b(t)]\boldsymbol{\varepsilon} - (1-v_h)\boldsymbol{e}_f\boldsymbol{E}, \qquad (2.10)$$

where $\boldsymbol{c}_h$ is the stiffness of the fluid phase, $\boldsymbol{c}_f$ is the stiffness of the oriented collagen fiber, $\boldsymbol{e}_f = \boldsymbol{e}$ denotes the electromechanical coupling coefficient matrix due to piezoelectricity in the collagen fibers. Here we introduce the influence of the bacterial growth in the stress generation through the bacterial concentration $b(t)$, where α denotes the volume occupied by the bacterial cells within the RVE. Equation (2.1b) takes the form

$$\boldsymbol{D} = [v_h\boldsymbol{\epsilon}_h + (1-v_h)\boldsymbol{\epsilon}_f]\boldsymbol{E} + (1-v_h)\boldsymbol{e}^T\boldsymbol{\varepsilon} + \epsilon_0\boldsymbol{\chi}(\omega_j)\boldsymbol{E}, \qquad (2.11)$$

where ϵ_0 is the dielectric constant of air, $\boldsymbol{\epsilon}_h$ and $\boldsymbol{\epsilon}_f$ are, respectively, the electric permittivity for fluid phase and the collagen fibers, $\boldsymbol{\chi}(\omega_j)$ is the electric susceptibility due to the potentially active macromolecules if present in the RVE with resonant frequencies ω_j. Setting $\boldsymbol{M} = 0$ in (2.1c) leads to $\boldsymbol{B} = \mu\boldsymbol{H}$. In our numerical simulation, we drop the above molecular susceptibility term due to unavailability of experimental data. To this end, we further simplify the general anisotropic nature of the constitutive model by neglecting certain elastic constants and certain electromechanical coupling terms, which gives finally the constitutive equations in the following matrix-vector form:

$$\begin{Bmatrix} \sigma_{xx} \\ \sigma_{yy} \\ \sigma_{zz} \\ \sigma_{yz} \\ \sigma_{zx} \\ \sigma_{xy} \end{Bmatrix} = \begin{bmatrix} c_{11} & c_{12} & c_{13} & 0 & 0 & c_{16} \\ c_{21} & c_{22} & c_{23} & 0 & 0 & c_{26} \\ c_{31} & c_{32} & c_{33} & 0 & 0 & c_{36} \\ 0 & 0 & 0 & c_{44} & c_{45} & 0 \\ 0 & 0 & 0 & c_{54} & c_{55} & 0 \\ c_{16} & c_{26} & c_{36} & 0 & 0 & c_{66} \end{bmatrix} \begin{Bmatrix} \varepsilon_{xx} \\ \varepsilon_{yy} \\ \varepsilon_{zz} \\ \varepsilon_{yz} \\ \varepsilon_{zx} \\ \varepsilon_{xy} \end{Bmatrix}$$
$$- \begin{bmatrix} 0 & 0 & 0 & 0 & 0 & 0 \\ 0 & 0 & 0 & 0 & 0 & 0 \\ e_{31} & e_{32} & e_{33} & 0 & 0 & e_{36} \end{bmatrix}^T \begin{Bmatrix} E_x \\ E_y \\ E_z \end{Bmatrix}, \qquad (2.12)$$

where

$$e_{ij} = c_{jk}d_{ik} \qquad (2.13)$$

with Einstein's summation in tensorial index k. Having obtained an explicit form of the constitutive model, the electromechanical conservation equations are derived in the next section.

In context of (2.10) and (2.11), note that we have introduced the effect of bacterial cells or antibiotic agents through the variable $b(t)$. For simplicity, it is assumed here that these external agents do not alter the electrical polarization properties of the macromolecules responsible for piezoelectricity. However, such an assumption may not hold

in real situations and a more detailed model may need to be developed in such cases. On the other hand, introduction of the variable $b(t)$ can also be useful in analyzing the long-term remodelling of site-specific collagen structure. The associated evolution law can be written as

$$\frac{\partial b}{\partial t} = \boldsymbol{\nabla}\left(\mathscr{D}(b)\boldsymbol{\nabla}b\right) + \beta n_d b - \mu_d b, \tag{2.14}$$

where the first term in the right-hand side represents the remodelling mechanism of bacterial cell movement with $\mathscr{D}(b) = \mathscr{D}_0 b^k$, $k > 0$, and $\mathscr{D}_0$ constants. The second term represents the dosimetric effect, that is, consumption of nutrients with concentration $n_d(\boldsymbol{x}, t)$ and β a nutrient-cell conversion factor. The third term represents formation of stationary cell-tissue structure. A detailed experimental observation of bacterial growth in chemically inert environment based on the above evolution law can be found in [1]. Since not much detailed information related to corneal collagen growth or dosimetric parameters is available, in the present study we do not couple (2.14) in the computational model, but assume various spatiotemporal states of b in (2.10) with the following distribution:

$$b(r, \theta, t) = \alpha'(t) e^{-k'(R-r)}\left[1 - \alpha'' e^{-k''(\theta^2 - \theta_0^2)}\right], \tag{2.15}$$

where (r, θ) are the polar coordinates in the projected plane, R is the radius of the corneal anterior on the projected plane, θ_0 is the angular orientation of the active site, $\alpha'(t)$ is prescribed at a given time assuming a different time scale for growth as compared to the dehydration, and k', α'', k'' are constants.

3. Dynamic piezoelectricity

The momentum conservation equation is derived in the usual manner, which is given by

$$\rho \frac{\partial^2 \boldsymbol{u}}{\partial t^2} - \boldsymbol{\nabla} \cdot (\boldsymbol{c}\boldsymbol{\nabla}\boldsymbol{u}) = \boldsymbol{f}(\boldsymbol{\nabla}E), \tag{3.1}$$

where the effective mass density is

$$\rho = v_h \rho_h + (1 - v_h)\rho_f, \tag{3.2}$$

and the components of the right-hand electrical source term are written as

$$f_x = -e_{31}\frac{\partial E_z}{\partial x} - e_{36}\frac{\partial E_z}{\partial y}, \qquad f_y = -e_{36}\frac{\partial E_z}{\partial x} - e_{32}\frac{\partial E_z}{\partial y}, \qquad f_z = -e_{33}\frac{\partial E_z}{\partial y}. \tag{3.3a}$$

We note that $\boldsymbol{f}$ is a function of only the transverse electric field E_z. This is due to the particular form of electromechanical coupling assumed in (2.12). For practical applications, this is a reasonably simple type of electromechanical coupling, yet an important one to analyze the direct influence of piezoelectricity on the refraction of incident ray $E_z \to E_\perp$ at

the outer surface $z = h_o$, with the constitutive model defined in (x, y, z) and transformed to $(x, y, z_\perp)$, where the subscript $\perp$ denotes the outer surface normal. In the finite-element computations that follow, the deformations at the surfaces and at the annular base (see Figure 2.1) have to satisfy the appropriate boundary conditions in a weak sense.

The transverse electric field in (3.3a) has to satisfy Maxwell's equations for the electromagnetic field:

$$\nabla \times \boldsymbol{E} = -\dot{\boldsymbol{B}}, \tag{3.4a}$$

$$\nabla \times \boldsymbol{H} = \dot{\boldsymbol{D}} + \sigma_c \boldsymbol{E} + \boldsymbol{J}, \tag{3.4b}$$

$$\nabla \cdot \boldsymbol{D} = \rho_c, \tag{3.4c}$$

$$\nabla \cdot \boldsymbol{B} = 0, \tag{3.4d}$$

where σ_c is the effective conductivity of the RVE. The associated general impedance boundary conditions (GIBCs) are

$$\boldsymbol{n} \times (\boldsymbol{E} - \boldsymbol{E}_\perp) = -\boldsymbol{J}_{sm}, \qquad \boldsymbol{n} \times (\boldsymbol{H} - \boldsymbol{H}_\parallel) = \boldsymbol{J}_s \tag{3.5a}$$

at surfaces $z_\perp = h_o, h_i$, and

$$\boldsymbol{n} \cdot \boldsymbol{D} = \rho_s, \qquad \boldsymbol{n} \cdot \boldsymbol{B} = 0 \tag{3.5b}$$

at the annular base near the corneal anterior and scleral interface with ρ_s as the surface charge, $\boldsymbol{n}$ is the unit outward surface normal.

By using the constitutive model derived in Section 2, Maxwell's equations in (3.4a)–(3.4d) are combined into the following system of coupled hyperbolic equations:

$$\mu\epsilon \frac{\partial^2 \boldsymbol{E}}{\partial t^2} + \sigma_c \mu \frac{\partial \boldsymbol{E}}{\partial t} - \nabla^2 \boldsymbol{E} + \mu \boldsymbol{e}^T \frac{\partial^2 \boldsymbol{\varepsilon}}{\partial t^2} - \boldsymbol{\epsilon}^{-1} \nabla \nabla \cdot (\boldsymbol{e}^T \boldsymbol{\varepsilon}) = \boldsymbol{\epsilon}^{-1} \nabla \rho_c + \mu \dot{\boldsymbol{J}}, \tag{3.6a}$$

$$\mu\epsilon \frac{\partial^2 \boldsymbol{H}}{\partial t^2} + \sigma_c \mu \frac{\partial \boldsymbol{H}}{\partial t} - \nabla^2 \boldsymbol{H} - \nabla \times \left(\boldsymbol{e}^T \frac{\partial \boldsymbol{\varepsilon}}{\partial t} \right) = -\nabla \times \boldsymbol{J}, \tag{3.6b}$$

where the right-hand-side terms in (3.6a)-(3.6b) are governed by the equation of the conduction of true charge, that is,

$$\nabla \cdot \boldsymbol{J} = -\rho_c. \tag{3.7}$$

In the finite-element simulations reported next, we have omitted the conduction part, for the sake of simplicity, while analyzing the direct piezoelectric effect. Due to this

simplification, we finally have

$$\mu \boldsymbol{\epsilon} \frac{\partial^2 \boldsymbol{E}}{\partial t^2} + \sigma_c \boldsymbol{\mu} \frac{\partial \boldsymbol{E}}{\partial t} - \nabla^2 \boldsymbol{E} = \boldsymbol{g}^E(\partial_{tt}, \nabla, \boldsymbol{\varepsilon}), \tag{3.8a}$$

$$\mu \boldsymbol{\epsilon} \frac{\partial^2 \boldsymbol{H}}{\partial t^2} + \sigma_c \boldsymbol{\mu} \frac{\partial \boldsymbol{H}}{\partial t} - \nabla^2 \boldsymbol{H} = \boldsymbol{g}^H(\partial_t, \nabla, \boldsymbol{\varepsilon}), \tag{3.8b}$$

where the components of the right-hand-side source terms, which are coupled with (3.1), are given by

$$g_x^E = \epsilon_{11}^{-1} \frac{\partial^2 \bar{P}}{\partial x \partial z}, \qquad g_y^E = \epsilon_{22}^{-1} \frac{\partial^2 \bar{P}}{\partial y \partial z}, \qquad g_z^E = \epsilon_{33}^{-1} \frac{\partial^2 \bar{P}}{\partial^2 z} - \mu_{33} \frac{\partial^2 \bar{P}}{\partial t^2}, \tag{3.9a}$$

$$g_x^H = \frac{\partial^2 \bar{P}}{\partial y \partial t}, \qquad g_y^H = -\frac{\partial^2 \bar{P}}{\partial x \partial t}, \qquad g_z^H = 0, \tag{3.9b}$$

and $\bar{P}$ is the effective polarization (a scalar quantity) due to piezoelectricity, which is given by

$$\bar{P} = e_{31}\varepsilon_{xx} + e_{32}\varepsilon_{yy} + e_{33}\varepsilon_{zz} + e_{36}\varepsilon_{xy}. \tag{3.10}$$

We solve the coupled system of hyperbolic equations (3.1), (3.8a), and (3.8b), supplemented by associated boundary conditions in $\{\boldsymbol{u}, \boldsymbol{E}, \boldsymbol{H}\}$ by using a three-dimensional finite-element discretization of the domain shown in Figure 2.1(a). COMSOL has been used for the solution where the constitutive model and the coupled system of equations have been implemented with the boundary conditions as weak constraints. Tetrahedral Lagrangian finite-elements and the second-order accurate time-stepping scheme have been used for computation.

4. Results and discussions

For numerical simulations, we consider a model of (x, y) cut of the corneal section as shown in Figure 2.1(a). It contains most of the usual geometric features with inner radius 5.685 mm and outer radius 7.259 mm. The conic-angle at the focal point is assumed to be $2 \times 59.434°$ with $h_i = 2.794$ mm, $h_0 - h_i = 0.449$ mm at $(x, y) = (0, 0)$. Thickness at the annular base is assumed to be 1.574 mm. A 100 Hz harmonic shear stress with amplitude of 10 MPa is applied at the base along x. A residual stress pattern over a circumferential arc segment can also be used to study the effect of incision. Figures 4.1(a) and 4.1(b), respectively, show the deformation contours without any circumferential activity and with bacterial growth, $\alpha\alpha' = 0.1$, $k' = 10/R$, $\alpha'' = 0$. The contour of transverse electric field in Figure 4.2 reveals the possible regions of refractive property modification as under the deformation pattern shown in Figure 4.1(b). Attention has been paid to avoid the spurious effect due to mesh discretization error. The results presented here have been obtained for a refined mesh with 11987 tetrahedral elements and nonuniform time-stepping set by the direct nonsymmetric sparse matrix solver used. It can be seen from Figure 4.1(b) that
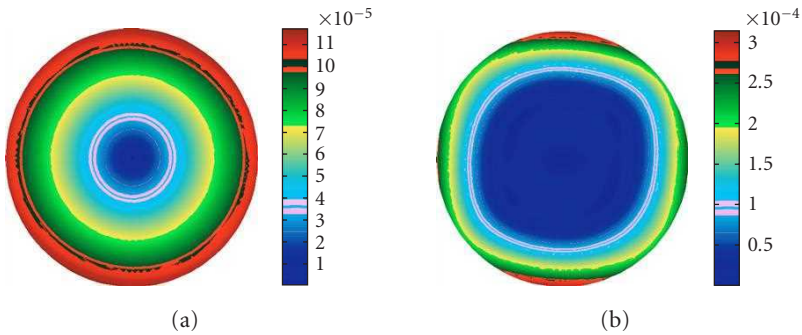
Figure 4.1. Deformation contours ($\sqrt{u_1^2 + u_2^2}$) for (a) symmetric circumferential stress distribution with $\alpha'' = 0$, (b) circumferential stress distribution with $\alpha'' = 0.9$.
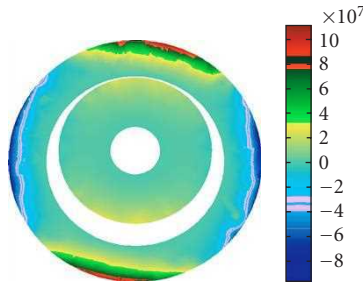

Figure 4.2. Sliced contour of transverse electric field E_3.

the residual stress at the circumferences due to bacterial growth (or incision) significantly alters the deformation profile and this observation is in close agreement with the studies reported in [6]. Further detailed analysis of the realistic situation of tunneling incision and astigmatism will be studied based on the present model in future research.

References

[1] E. Ben-Jacob, I. Cohen, I. Golding, D. L. Gutnick, M. Tcherpakov, D. Helbing, and I. G. Ron, *Bacterial cooperative organization under antibiotic stress*, Physica A **282** (2000), no. 1-2, 247–282.

[2] E. Fukuda and I. Yasuda, *Piezoelectric effect in collagen*, Journal of Applied Physics **3** (1964), no. 2, 117–121.

[3] M. T. Girard, M. Matsubara, C. Kublin, M. J. Tessler, C. Cintron, and M. E. Fini, *Stromal fibroblasts synthesize collagens and stromelysin during long-term tissue remodelling*, Journal of Cell Science **104** (1993), no. 4, 1001–1011.

[4] A. C. Jayasuriya, S. Ghosh, J. I. Scheinbeim, V. Lubkin, G. Bennett, and P. Kramer, *A study of piezoelectric and mechanical anisotropy of the human cornea*, Biosensors and Bioelectronics **18** (2003), 381–387.

[5] W. M. Petroll, L. Ma, and V. Jester, *Direct correlation of collagen matrix deformation with focal adhesion dynamics in living corneal fibroblasts*, Journal of Cell Science **116** (2003), 1489–1491.

[6] P. M. Pinsky, D. van der Heide, and D. Chernyak, *Computational modelling of mechanical anisotropy in the cornea and sclera*, Journal of Cataract & Refractive Surgery **31** (2005), no. 1, 136–145.

[7] P. Pratzl and A. Daxer, *Structural transformation of collagen fibrils in corneal stroma during drying*, Biophysical Journal **64** (1993), no. 4, 1210–1214.

[8] M. H. Shamos and L. S. Lavine, *Piezoelectricity as a fundamental property of biological tissues*, Nature **213** (1967), no. 73, 267–269.

D. Roy Mahapatra: Mathematical Modelling and Computational Sciences, Wilfrid Laurier University, Waterloo, ON, Canada N2L 3C5
E-mail address: droymahapatra@wlu.ca

R. V. N. Melnik: Mathematical Modelling and Computational Sciences, Wilfrid Laurier University, Waterloo, ON, Canada N2L 3C5
E-mail address: rmelnik@wlu.ca